Published for SISSA by Springer

Received: October 24, 2012
Accepted: December 10, 2012
Published: January 16, 2013

A study of the Z production cross-section in pp collisions at $\sqrt{s} = 7$ TeV using tau final states

The LHCb collaboration

Abstract: A measurement of the inclusive $Z \to \tau\tau$ cross-section in pp collisions at $\sqrt{s} = 7$ TeV is presented based on a dataset of 1.0 fb^{-1} collected by the LHCb detector. Candidates for $Z \to \tau\tau$ decays are identified through reconstructed final states with two muons, a muon and an electron, a muon and a hadron, or an electron and a hadron. The production cross-section for Z bosons, with invariant mass between 60 and 120 GeV/c^2, which decay to τ leptons with transverse momenta greater than 20 GeV/c and pseudorapidities between 2.0 and 4.5, is measured to be $\sigma_{pp\to Z\to\tau\tau} = 71.4 \pm 3.5 \pm 2.8 \pm 2.5$ pb; the first uncertainty is statistical, the second is systematic, and the third is due to the uncertainty on the integrated luminosity. The ratio of the cross-sections for $Z \to \tau\tau$ to $Z \to \mu\mu$ is determined to be 0.93 ± 0.09, where the uncertainty is the combination of statistical, systematic, and luminosity uncertainties of the two measurements.

Keywords: Hadron-Hadron Scattering

ArXiv ePrint: 1210.6289

doi:10.1007/JHEP01(2013)111

JHEP01(2013)111

Contents

1 Introduction 1

2 Detector and datasets 2

3 Event selection 2

4 Background estimation 4

5 Cross-section measurement 6

5.1 Acceptances and branching fractions 7

5.2 Selection efficiency 7

5.3 Reconstruction efficiency 8

6 Results 10

7 Conclusions 12

The LHCb collaboration 16

JHEP01(2013)111

1 Introduction

The measurement of the production cross-section for Z bosons[1] in proton-proton (pp) collisions constitutes an important verification of Standard Model predictions. Since lepton universality in Z decays has been tested to better than 1% at LEP [1], any deviation observed at the LHC would be evidence for additional physics effects producing final state leptons. In particular, τ-lepton pairs can be important signatures for supersymmetry, extra gauge bosons, or extra dimensions [2–4]. The LHCb experiment has previously measured the cross-section for $Z \to \mu\mu$ [5] with both leptons having transverse momentum ($p_{\rm T}$) above 20 GeV/c and an invariant mass between 60 and 120 GeV/c^2. Here a complementary measurement in the decay mode $Z \to \tau\tau$ is presented. This measurement extends the $Z \to \tau\tau$ cross-section measurements from the central pseudorapidity range covered by ATLAS ($|\eta| < 2.4$) [6] and CMS ($|\eta| < 2.3$) [7] into the forward region covered by the LHCb experiment ($2 < \eta < 4.5$).

[1] Here, the Z is used to indicate production from Z bosons, photons, and their interference.

2 Detector and datasets

The LHCb detector [8] is a single-arm forward spectrometer designed for the study of particles containing b or c quarks. The detector includes a high precision tracking system consisting of a silicon-strip vertex detector (VELO) surrounding the pp interaction region, a large-area silicon-strip detector (TT) located upstream of a dipole magnet with a bending power of about 4 Tm, and three stations of silicon-strip detectors (IT) and straw drift tubes (OT) placed downstream. The combined tracking system has a momentum resolution $\Delta p/p$ that varies from 0.4% at 5 GeV/c to 0.6% at 100 GeV/c, and an impact parameter resolution of 20 μm for tracks with high $p_{\rm T}$.

Charged hadrons are identified using two ring-imaging Cherenkov detectors. Photon, electron and hadron candidates are identified by a calorimeter system consisting of scintillating-pad (SPD) and pre-shower detectors (PRS), an electromagnetic calorimeter (ECAL) and a hadronic calorimeter (HCAL). Muons are identified by a system composed of alternating layers of iron and multiwire proportional chambers. The trigger consists of a hardware stage, based on information from the calorimeter and muon systems, followed by a software stage that applies a full event reconstruction. The hardware stage imposes a global event requirement (GEC) on the hit multiplicities of most sub-detectors used in the pattern recognition algorithms to avoid overloading of the software trigger by high occupancy events.

This analysis uses data, corresponding to an integrated luminosity of 1028 ± 36 pb^{-1}, taken at a centre-of-mass energy of 7 TeV. The absolute luminosity scale was measured periodically throughout the data taking period using Van der Meer scans [9] where the beam profile is determined by moving the beams transversely across one another. A beam-gas imaging method was also used where the beam profile is determined through reconstructing beam-gas interaction vertices near the beam crossing point [10]. Both methods provide similar results and the integrated luminosity is determined from the average of the two, with an estimated systematic uncertainty of 3.5% [11]. The primary systematic uncertainty of 2.7% is due to the beam current measurement, shared between the two methods.

Simulated data samples are used to develop the event selection, determine efficiencies, and estimate systematic uncertainties. Each sample was generated using an LHCb configuration [12] of Pythia 6.4 [13] with the CTEQ6L1 leading-order PDF set [14] and passed through a Geant4 [15, 16] based simulation of the LHCb detector [17]. Trigger emulation and full event reconstruction were performed using the LHCb reconstruction software [18]. Additional samples, without detector simulation or event reconstruction, are used to study the signal acceptance and were generated using Pythia 8.1.55 [19], Herwig++ 2.5.1 [20], and Herwig++ with the Powheg method [21].

3 Event selection

The signatures for $Z \to \tau\tau$ decays considered in this analysis are two oppositely-charged tracks, consistent with an electron, muon, or hadron hypothesis, having large impact parameters with respect to the primary vertex of the event.

JHEP01(2013)111

Tracks are reconstructed in the VELO and extrapolated to the IT/OT sub-detectors; any TT sub-detector hits consistent with the track are added and a full track fit is performed. Only tracks with fit probabilities greater than 0.001 are considered.

Tracks are extrapolated to the calorimeters and matched with calorimeter clusters. Electron candidates are required to have a PRS energy greater than 0.05 GeV, a ratio of ECAL energy to candidate momentum, E/pc, greater than 0.1, and a ratio of HCAL energy to candidate momentum less than 0.05. Any electron candidate momentum is corrected using bremsstrahlung photon recovery [22]. Since the ECAL is designed to register particles from b-hadron decays, calorimeter cells with transverse energy above 10 GeV saturate the electronics, and lead to degradation in the electron energy resolution.

Hadron candidates are identified by requiring the ratio of HCAL energy to track momentum to be greater than 0.05. Due to the limited HCAL acceptance, the candidate track is required to have a pseudorapidity of $2.25 \leq \eta \leq 3.75$.

Muon candidates are identified by extrapolating tracks to the muon system downstream of the calorimeters and matching them with compatible hits. Muon candidates are required to have a hit in each of the four stations and consequently will have traversed over 20 hadronic interaction lengths of material.

The data have been collected using two triggers: a trigger which selects muon candidates with a p_{T} greater than 10 GeV/c; and a trigger which selects electron candidates with p_{T} greater than 15 GeV/c.

The analysis is divided into five streams, labelled $\tau_\mu\tau_\mu$, $\tau_\mu\tau_e$, $\tau_e\tau_\mu$, $\tau_\mu\tau_h$, and $\tau_e\tau_h$, defined such that the streams are exclusive. The first τ lepton decay product candidate is required to have $p_{\mathrm{T}} > 20$ GeV/c and the second is required to have $p_{\mathrm{T}} > 5$ GeV/c. The following additional kinematic and particle identification requirements are specific to each analysis stream:

- $\tau_\mu\tau_\mu$ requires two oppositely-charged muons where at least one triggered the event. The muon with the larger p_{T} is considered as the first τ lepton decay product candidate.
- $\tau_\mu\tau_e$ requires a muon that triggered the event and an oppositely-charged electron.
- $\tau_e\tau_\mu$ requires an electron and an oppositely-charged muon with $p_{\mathrm{T}} < 20$ GeV/c. Either lepton can trigger the event.
- $\tau_\mu\tau_h$ requires a muon that triggered the event and an oppositely-charged hadron.
- $\tau_e\tau_h$ requires an electron that triggered the event and an oppositely-charged hadron.

In pp collisions the cross-section for hadronic QCD processes is very large. These events can pass the above requirements either due to semileptonic c- or b-hadron decays or through the misidentification of hadrons as leptons.

Signal decays, coming from an on-shell Z, tend to have back-to-back isolated tracks in the transverse plane with a higher invariant mass than tracks in QCD events. The absolute difference in azimuthal angle of the two τ lepton decay product candidates, $|\Delta\Phi|$, is required to be greater than 2.7 radians and their invariant mass is required to be greater than 20 GeV/c^2.

JHEP01(2013)111

Tracks in QCD events also tend to be associated with jet activity, in contrast to signal events where they are isolated. An isolation variable, $I_{p_{\mathrm{T}}}$, is defined as the transverse component of the vectorial sum of all track momenta that satisfy $\sqrt{\Delta\phi^2 + \Delta\eta^2} < 0.5$, where $\Delta\phi$ and $\Delta\eta$ are the differences in ϕ and η between the τ lepton decay product candidate and the track. The track of the τ lepton decay product candidate is excluded from the sum. Both τ lepton decay product candidates are required to have $I_{p_{\mathrm{T}}} < 2$ GeV/c for the $\tau_\mu\tau_\mu$, $\tau_\mu\tau_e$, and $\tau_e\tau_\mu$ analysis streams and $I_{p_{\mathrm{T}}} < 1$ GeV/c for $\tau_\mu\tau_h$ and $\tau_e\tau_h$ due to the larger QCD backgrounds.

The lifetime of the τ lepton is used to separate signal from prompt backgrounds. The signed impact parameter for a track is defined as the magnitude of the track vector of closest approach to the primary vertex signed by the z-component of the cross product between this vector and the track momentum. The impact parameter significance, IPS, is then defined as the absolute sum of the signed impact parameters of the two τ lepton decay product candidates, divided by their combined uncertainty. The IPS is required to be greater than 9 for the $\tau_\mu\tau_\mu$, $\tau_\mu\tau_h$, and $\tau_e\tau_h$ analysis streams while no IPS requirement is placed on the $\tau_\mu\tau_e$ or $\tau_e\tau_\mu$ streams.

In the $\tau_\mu\tau_\mu$ analysis stream an additional background component arises from $Z \to \mu\mu$ events. This produces two muons with similar p_{T}, most of which also have an invariant mass close to the Z mass. In contrast, signal events tend to have unbalanced p_{T} and a lower invariant mass due to unreconstructed energy from neutrinos and neutral hadrons. The p_{T} asymmetry, $A_{p_{\mathrm{T}}}$, is defined as the absolute difference between the p_{T} of the two candidates divided by their sum. For the $\tau_\mu\tau_\mu$ analysis stream the $A_{p_{\mathrm{T}}}$ is required to be greater than 0.3 and the di-muon invariant mass must lie outside the range $80 < M_{\mu\mu} < 100$ GeV/c^2.

4 Background estimation

The invariant mass distributions for the selected $Z \to \tau\tau$ candidates, the simulated signal, and the estimated backgrounds for the five analysis streams are shown in figure 1, where no candidates are observed with a mass above 120 GeV/c^2. Five types of background have been considered: generic QCD; electroweak, where a high p_{T} lepton is produced by a W or Z boson and the second candidate τ lepton decay product is misidentified from the underlying event; $t\bar{t}$, where two hard leptons are produced from top decays; WW, where each W decays to a lepton; and $Z \to \ell\ell$ for the $\tau_\mu\tau_\mu$, $\tau_\mu\tau_h$, and $\tau_e\tau_h$ streams, where for the $\tau_\mu\tau_h$ stream a single muon is misidentified as a hadron and for the $\tau_e\tau_h$ stream an electron is misidentified. The $t\bar{t}$ and WW backgrounds are estimated using simulation and found to be small for all final states.

The QCD and electroweak backgrounds are estimated from data. A signal-depleted control sample is created by applying all selection criteria but requiring that the τ lepton decay product candidates have the same-sign (SS) charge. The QCD and electroweak background events in this sample, $N^{\mathrm{SS}}_{\mathrm{QCD}}$ and $N^{\mathrm{SS}}_{\mathrm{EWK}}$, are obtained by fitting template shapes to the distribution of the difference between the p_{T} of the first and second τ lepton decay product candidates. The template shape for the electroweak background is taken from simulation. To determine the shape of the QCD contribution, the isolation requirement is

JHEP01(2013)111

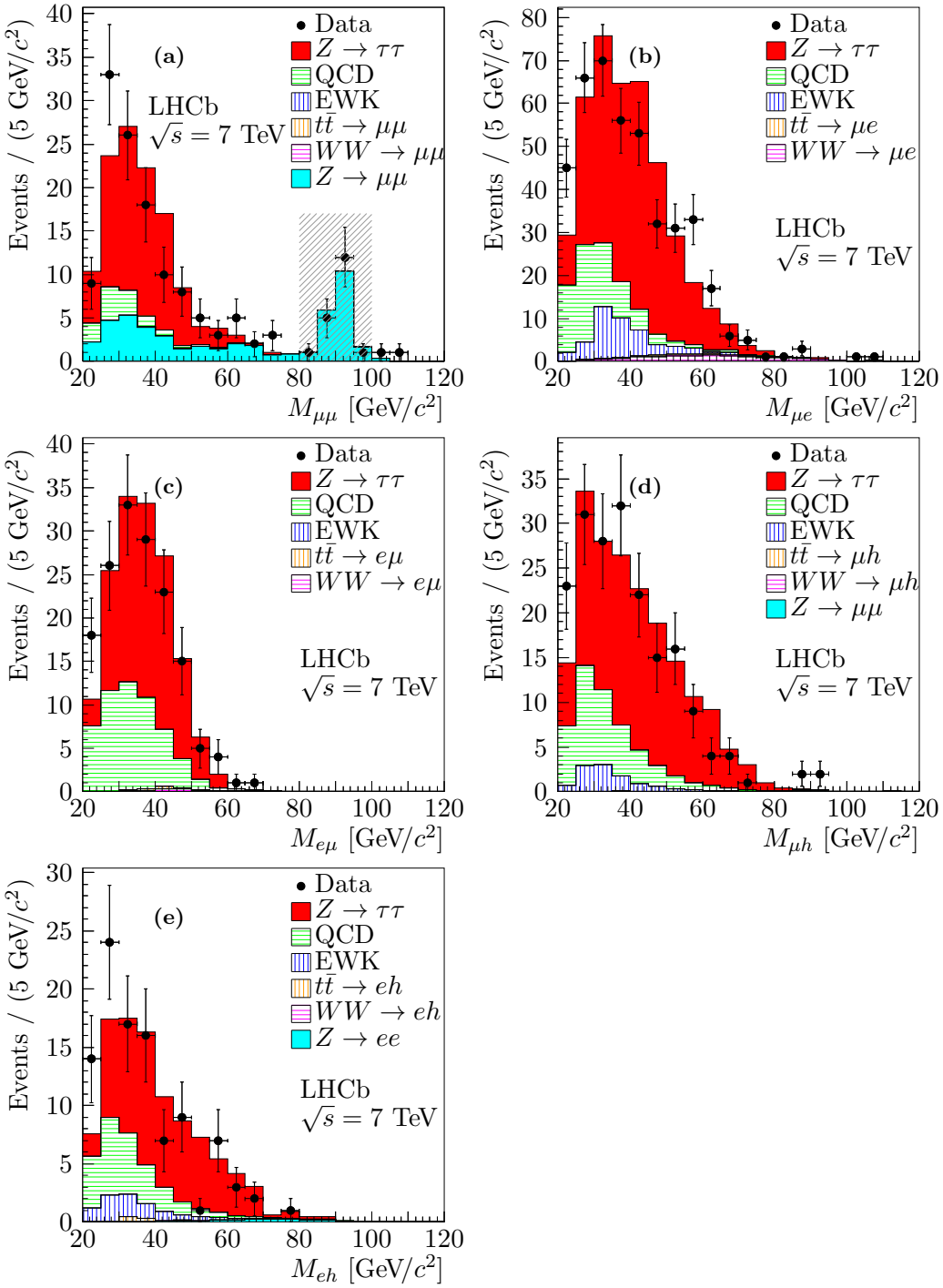

Figure 1. Invariant mass distributions for the (a) $\tau_\mu\tau_\mu$, (b) $\tau_\mu\tau_e$, (c) $\tau_e\tau_\mu$, (d) $\tau_\mu\tau_h$, and (e) $\tau_e\tau_h$ candidates with the excluded mass range indicated for $\tau_\mu\tau_\mu$. The $Z \to \tau\tau$ simulation (solid red) is normalised to the number of signal events. The QCD (horizontal green), electroweak (vertical blue), and Z (solid cyan) backgrounds are estimated from data. The $t\bar{t}$ (vertical orange) and WW (horizontal magenta) backgrounds are estimated from simulation and generally not visible.

JHEP01(2013)111

reversed such that $I_{p_T} > 10$ GeV/c. The number of candidates for each background category in the signal sample is then calculated as $N_{\rm QCD} = f_{\rm QCD} N^{\rm SS}_{\rm QCD}$ and $N_{\rm EWK} = f_{\rm EWK} N^{\rm SS}_{\rm EWK}$, where $f_{\rm QCD}$ and $f_{\rm EWK}$ are the ratio of opposite-sign to same-sign events for QCD and electroweak events respectively. Both $f_{\rm QCD}$ and $f_{\rm EWK}$ are determined as the ratio of opposite-sign to same-sign events satisfying the template requirements. The uncertainties on the QCD and electroweak backgrounds are estimated by combining the statistical uncertainty on the fraction with the uncertainties from the fit used to determine $N^{\rm SS}_{\rm QCD}$ and $N^{\rm SS}_{\rm EWK}$.

The number of $Z \to \mu\mu$ background events for the $\tau_\mu\tau_\mu$ stream is obtained by applying all selection criteria except for the $80 < M_{\mu\mu} < 100$ GeV/c^2 requirement. This produces a sample with a clear peak around the Z mass as shown in figure a. A template for $Z \to \mu\mu$ events is obtained from data by applying the event selection, but requiring prompt events with IPS < 1. The template is normalised to the number of events within the $\tau_\mu\tau_\mu$ sample with IPS > 9 and within the invariant mass range $80 < M_{\mu\mu} < 100$ GeV/c^2. The $Z \to \mu\mu$ background is the number of events in the normalised template outside this mass range. The uncertainty on this background is estimated from the statistical uncertainty on the normalisation factor.

The $Z \to \mu\mu$ process also contributes a small background to the $\tau_\mu\tau_h$ stream when one of the muons is misidentified as a hadron. This is evaluated by applying the $\tau_\mu\tau_h$ selection but requiring a second identified muon rather than a hadron, and scaling this by the probability for a muon to be misidentified as a hadron. The latter is found from a sample of $Z \to \mu\mu$ events that have been selected by requiring a single well defined muon and a second isolated track, which give an invariant mass between 80 and 100 GeV/c^2; $(0.06 \pm 0.01)\%$ of these tracks pass the hadron identification requirement.

Similarly, a small $Z \to ee$ background can contribute to the $\tau_e\tau_h$ stream when one of the electrons is misidentified as a hadron. This is evaluated by applying the $\tau_e\tau_h$ selection but requiring a second identified electron rather than a hadron, and scaling this by the probability for an electron to be misidentified as a hadron. The electron mis-identification is found from simulated $Z \to ee$ events to be $(0.63 \pm 0.02)\%$.

5 Cross-section measurement

The $pp \to Z \to \tau\tau$ cross-section is calculated within the kinematic region $60 < M_{\tau\tau} < 120$ GeV/c^2, $2.0 \leq \eta^\tau \leq 4.5$, and $p^\tau_{\rm T} > 20$ GeV/c using

$$\sigma_{pp\to Z\to\tau\tau} = \frac{\sum_{i=1}^{N} 1/\varepsilon^i_{\rm rec} - \sum_j N^j_{\rm bkg} \langle 1/\varepsilon_{\rm rec}\rangle^j}{\mathscr{L} \cdot \mathcal{A} \cdot \mathcal{B} \cdot \varepsilon_{\rm sel}} \tag{5.1}$$

where N is the number of observed candidates and $N^j_{\rm bkg}$ is the estimated background from source j. The integrated luminosity is given by $\mathscr{L}$, $\mathcal{A}$ is an acceptance and final state radiation correction factor, $\mathcal{B}$ is the branching fraction for the τ-lepton pair to decay to the final state, and $\varepsilon_{\rm sel}$ is the selection efficiency. A summary of these values for each final state is given in table 1. The reconstruction efficiency, $\varepsilon_{\rm rec}$, is calculated using simulation or data for each event, assuming that it is signal, and depends on the momentum and

JHEP01(2013)111

Stream	$\mathcal{A}$	$\mathcal{B}$ [%]	ε_{sel}	N_{bkg}	N
$\tau_\mu\tau_\mu$	0.405 ± 0.006	3.031 ± 0.014	0.138 ± 0.006	41.6 ± 8.5	124
$\tau_\mu\tau_e$	0.248 ± 0.004	6.208 ± 0.020	0.517 ± 0.012	129.7 ± 4.9	421
$\tau_e\tau_\mu$	0.152 ± 0.002	6.208 ± 0.020	0.344 ± 0.016	56.6 ± 3.3	155
$\tau_\mu\tau_h$	0.182 ± 0.002	16.933 ± 0.056	0.135 ± 0.004	53.3 ± 0.8	189
$\tau_e\tau_h$	0.180 ± 0.002	17.341 ± 0.057	0.082 ± 0.004	36.6 ± 0.9	101

Table 1. Acceptance factors, branching fractions, selection efficiencies, numbers of background and observed events for each $Z \to \tau\tau$ analysis stream.

pseudorapidity of the τ lepton decay product candidates. $\langle 1/\varepsilon_{\text{rec}} \rangle^j$ indicates the average value of $1/\varepsilon_{\text{rec}}$ for background source j.

The integrated luminosity of the datasets for the $\tau_\mu\tau_\mu$, $\tau_\mu\tau_e$, and $\tau_\mu\tau_h$ samples is 1028 ± 36 pb^{-1}, while the $\tau_e\tau_\mu$ and $\tau_e\tau_h$ final state datasets have an integrated luminosity of 955 ± 33 pb^{-1}.

5.1 Acceptances and branching fractions

The acceptance factor, $\mathcal{A}$, is used to correct the kinematics of each analysis stream to the kinematic region $60 < M_{\tau\tau} < 120$ GeV/c^2, $2.0 \leq \eta^\tau \leq 4.5$, and $p_{\text{T}}^\tau > 20$ GeV/c. This region corresponds to the detector fiducial acceptance and allows a comparison with the LHCb $Z \to \mu\mu$ measurement [5]. The acceptance factor is taken from simulation and is defined as the number of $Z \to \tau\tau$ events where the generated τ lepton decay products fulfil the kinematic requirements described in section 3, divided by the number of $Z \to \tau\tau$ events where the generated τ leptons lie within the kinematic region defined above.

For each final state the acceptance factors are calculated at leading-order using fully modelled hadronic decay currents and spin correlated τ lepton decays with final state radiation in Pythia 8 and Herwig++, and at next-to-leading-order using the Powheg method implemented in Herwig++. For Pythia 8 the CTEQ5L leading-order PDF set [23] was used, while for Herwig++ the MSTW08 PDF set [24] was used. The mean of the maximum and minimum values from the three generators is taken as the acceptance factor and is given in table 1. The uncertainty is taken as half the difference between the maximum and minimum values.

The branching fractions are calculated using the world averages [25] and are given in table 1. The τ lepton to single charged-hadron branching fraction is the sum of all τ lepton decays containing a single charged hadron. The final states presented in this analysis account for 44% of all expected $Z \to \tau\tau$ decays.

5.2 Selection efficiency

The event selection efficiency, ε_{sel}, is the product of the efficiencies described below. Each efficiency is determined from either data, or simulation which has been calibrated using data. The resulting ε_{sel} for each stream is given in table 1.

JHEP01(2013)111

The kinematic efficiency, $\varepsilon_{\rm kin}$, is obtained from simulation and is the number of events fulfilling the kinematic requirements of section 3 at both the simulated and reconstructed level divided by the number of events passing the requirements at the simulated level. The efficiency is consistent with unity for the $\tau_\mu\tau_\mu$ and $\tau_\mu\tau_h$ analysis streams. For streams involving electrons, $\varepsilon_{\rm kin}$ is significantly lower due to the saturation of the ECAL. This results in electrons being reconstructed with lower momenta than their true momenta due to incomplete bremsstrahlung recovery. In the $\tau_\mu\tau_e$, $\tau_e\tau_\mu$, and $\tau_e\tau_h$ streams, $\varepsilon_{\rm kin}$ is $(99.3\pm1.0)\%$, $(66.8\pm1.9)\%$, and $(67.0\pm1.3)\%$ respectively. The uncertainties come from the statistical uncertainty of the $Z\to\tau\tau$ simulation and the calibration of the electron momentum scale which has been obtained by comparing the $p_{\rm T}$ spectrum of $Z\to ee$ events in data and simulation [26].

The efficiency of the isolation requirement, $\varepsilon_{I_{p_{\rm T}}}$, for each analysis stream is taken from $Z\to\tau\tau$ simulation, and calibrated to data by multiplying $\varepsilon_{I_{p_{\rm T}}}$ by the ratio of the efficiency obtained in $Z\to\mu\mu$ data to $Z\to\tau_\mu\tau_\mu$ simulation. The systematic uncertainty on $\varepsilon_{I_{p_{\rm T}}}$ is estimated as the difference between the efficiencies obtained from $Z\to\mu\mu$ simulation and $Z\to\tau_\mu\tau_\mu$ simulation.

The efficiency of the impact parameter significance requirement, $\varepsilon_{\rm IPS}$, is evaluated from $Z\to\tau\tau$ simulation. A comparison of the IPS distributions in $Z\to\mu\mu$ events from data and simulation show that the impact parameter resolution is underestimated by $(12\pm1)\%$ in simulation, and so the simulated $Z\to\tau\tau$ events are corrected by this factor. The systematic uncertainty on $\varepsilon_{\rm IPS}$ is determined by re-calculating the efficiency in $Z\to\tau\tau$ simulation with the scale factor varied by its uncertainty.

The efficiency of the azimuthal angle separation requirement, $\varepsilon_{|\Delta\Phi|}$, and $p_{\rm T}$ asymmetry efficiency requirement, $\varepsilon_{A_{p_{\rm T}}}$, are evaluated from simulation. The systematic uncertainty on each is taken as the difference in the evaluation of these efficiencies in $Z\to\mu\mu$ data and simulation, combined in quadrature with the statistical uncertainty from the $Z\to\tau\tau$ simulation.

5.3 Reconstruction efficiency

The reconstruction efficiency, $\varepsilon_{\rm rec}$, is the product of the GEC, trigger, and tracking and identification efficiencies for both τ lepton decay product candidates. The tracking efficiency is the probability for reconstructing the track and the identification efficiency is the probability for the track to be identified by the relevant sub-detectors. All efficiencies determined from data have been checked against simulation and found to agree within the percent level.

The GEC efficiency, $\varepsilon_{\rm GEC}$, is a correction for the loss due to the rejection by the hardware trigger of events with an SPD multiplicity of greater than 600 hits. For muon triggered events, the efficiency has been evaluated to be $(95.5\pm0.1)\%$ from $Z\to\mu\mu$ data events using a hardware di-muon trigger with a relaxed SPD requirement of 900 hits. For electron trigger events, the efficiency is estimated to be $(95.1\pm0.1)\%$ by comparing the hit multiplicities in $Z\to\mu\mu$ and $Z\to ee$ events.

The muon and electron trigger efficiencies, $\varepsilon_{\rm trg}$, are evaluated in bins of momentum using a tag-and-probe method on $Z\to\ell\ell$ data events, which have been selected requiring

JHEP01(2013)111

two reconstructed and identified muon or electron candidates with an invariant mass consistent with that of the Z. In the events the triggered lepton is taken as the tag lepton, and the other as the probe lepton. The event topologies for $Z \to \ell\ell$ and $Z \to \tau\tau$ events are nearly identical except for the momenta of the final state particles and so the trigger efficiency is calculated only as a function of the probe momentum below 500 GeV/c. The trigger efficiency is the fraction of events where the probe has also triggered, and varies as a function of probe momentum between 75% and 80% for the muon trigger and between 62% and 75% for the electron trigger. The trigger efficiency uncertainty for each bin in momenta is taken as the statistical uncertainty.

The tracking efficiency, $\varepsilon_{\rm trk}$, is also evaluated for muons using a tag-and-probe method on the $Z \to \mu\mu$ data. The tag must satisfy all the muon reconstruction and identification requirements. The probe is reconstructed from a track segment in the muon chambers that has been associated to a hit in the TT sub-detector, which is not required in the track reconstruction. Events with a tag and probe mass consistent with the on-shell Z mass are used. The tracking efficiency is evaluated as the number of events with a reconstructed probe track over the total number of events. For lower $p_{\rm T}$ tracks, masses consistent with the J/ψ are used.

The $J/\psi \to \mu\mu$ topology differs from the $Z \to \tau\tau$ topology in both pseudorapidity and momentum, and so the J/ψ muon tracking efficiencies are evaluated in bins of both variables. The muon tracking efficiency is found to vary between 85% and 93%. The uncertainty on the tracking efficiency is given by the statistical precision and the knowledge of the purity of the sample of $J/\psi \to \mu\mu$ candidates. The purity is estimated by fitting the di-muon invariant mass distribution of the $J/\psi \to \mu\mu$ candidates with a Crystal Ball function [27] to describe the signal shape and a linear background. An alternative estimate is obtained by fitting only the linear background on either side of the di-muon resonance. The difference in the efficiency evaluated using the two purity methods is taken as the systematic uncertainty.

All particles pass through approximately 20% of a hadronic interaction length of material prior to the final tracking station. Early showering of hadrons reduces the hadron tracking efficiency compared to the muon tracking efficiency. An additional correction factor to the muon tracking efficiency of $(84.3 \pm 1.5)\%$ for hadrons is applied which has been estimated using the full detector simulation, where the uncertainty on this correction corresponds to an uncertainty of 10% in the material budget [28].

The electron tracking efficiency uses a tag-and-probe method on $Z \to ee$ data events. The tag must satisfy all the electron reconstruction and identification requirements and the probe is selected as the highest energy ECAL cluster in the event not associated with the tag. The purity of the sample is found, from simulation, to depend on the $p_{\rm T}$ of the tag. The dependence of the purity is fitted with signal and background templates obtained from same-sign and opposite-sign events from data. No momentum information is available for the probe, so the tag-and-probe technique only provides an overall tracking efficiency for the electrons, which is measured to be $(83 \pm 3)\%$. The momentum dependence is taken from $Z \to ee$ and $Z \to \tau\tau$ simulation. The electron tracking efficiency uncertainty is taken from the fit uncertainty added in quadrature to the statistical uncertainty.

JHEP01(2013)111

The identification efficiency, $\varepsilon_{\rm id}$, is measured for muons with the tag-and-probe method for the $Z \to \mu\mu$ data, using a reconstructed track as the probe lepton and evaluated as a function of the probe momentum. For low momenta the efficiency is evaluated using a $J/\psi \to \mu\mu$ sample as a function of both probe pseudorapidity and momentum. The muon identification efficiency is found to vary between 93% and 99% in pseudorapidity and momentum. The muon $\varepsilon_{\rm id}$ uncertainty is evaluated with the same method used for the muon $\varepsilon_{\rm trk}$ uncertainty.

The electron identification efficiency is measured as a function of probe momentum using the tag-and-probe method on $Z \to ee$ data and simulation events. The isolation requirement introduces a bias of $1\% - 4\%$ in data and reconstructed simulation and so simulation without the isolation criteria is used instead. The electron identification efficiency is found to vary between 85% and 96%, with an uncertainty in each bin estimated as the difference in the biased efficiencies from data and simulation.

The hadron identification efficiency is determined using events triggered on a single VELO track. The highest $p_{\rm T}$ track in each minimum bias event is assumed to be a hadron, as verified by simulation. The hadron identification efficiency is taken as the fraction of tracks fulfilling the hadron identification requirements. Although the minimum bias topology differs significantly from the $Z \to \tau\tau$ topology, an efficiency dependence is observed only in pseudorapidity and so the efficiency is evaluated as a function of pseudorapidity and found to vary between 92% and 95%. The uncertainty for each bin of pseudorapidity is estimated as the statistical uncertainty of the bin. A summary of the systematic uncertainties is given in table 2.

6 Results

The cross-sections for each analysis stream are determined using eq. (5.1), the values given in table 1, and the systematic uncertainties presented in table 2. The results are

$$\begin{aligned}
\sigma_{pp\to Z\to\tau\tau}\ (\tau_\mu\tau_\mu) &= 77.4 \pm 10.4 \pm 8.6 \pm 2.7 \text{ pb} \\
\sigma_{pp\to Z\to\tau\tau}\ (\tau_\mu\tau_e) &= 75.2 \pm \ 5.4 \pm 4.1 \pm 2.6 \text{ pb} \\
\sigma_{pp\to Z\to\tau\tau}\ (\tau_e\tau_\mu) &= 64.2 \pm \ 8.2 \pm 4.9 \pm 2.2 \text{ pb} \\
\sigma_{pp\to Z\to\tau\tau}\ (\tau_\mu\tau_h) &= 68.3 \pm \ 7.0 \pm 2.6 \pm 2.4 \text{ pb} \\
\sigma_{pp\to Z\to\tau\tau}\ (\tau_e\tau_h) &= 77.9 \pm 12.2 \pm 6.1 \pm 2.7 \text{ pb}
\end{aligned}$$

where the first uncertainty is statistical, the second uncertainty is systematic, and the third is due to the uncertainty on the integrated luminosity.

A global fit is performed using a best linear unbiased estimator [29] including correlations between the final states, and a combined result of

$$\sigma_{pp\to Z\to\tau\tau} = 71.4 \pm 3.5 \pm 2.8 \pm 2.5 \text{ pb}$$

is obtained, with a χ^2 per degree of freedom of 0.43. The statistical uncertainties are assumed to be uncorrelated as each analysis stream contains mutually exclusive datasets. The luminosity and any shared selection or reconstruction efficiencies are assumed to be fully correlated.

JHEP01(2013)111

Stream		$\Delta\sigma_{pp\to Z\to\tau\tau}$ [%]				
		$\tau_\mu\tau_\mu$	$\tau_\mu\tau_e$	$\tau_e\tau_\mu$	$\tau_\mu\tau_h$	$\tau_e\tau_h$
$\mathcal{A}$		1.48	1.61	1.32	1.10	1.11
$\mathcal{B}$		0.46	0.32	0.32	0.32	0.33
N_{bkg}	N_{QCD}	4.33	0.80	3.08	0.40	0.92
	N_{EWK}	4.22	1.54	1.52	0.40	0.72
	$N_{t\bar{t}}$	0.02	0.08	0.12	0.00	0.58
	N_{WW}	0.02	0.14	0.13	0.09	0.08
	N_Z	8.00	–	–	0.22	0.23
Total N_{bkg}		10.03	1.75	3.44	0.61	1.32
ε_{rec}	ε_{GEC}	0.10	0.10	0.10	0.10	0.10
	ε_{trg}	0.88	0.71	2.29	0.72	4.30
	${\varepsilon_{\text{trk}}}^{(1)}$	0.71	0.74	3.67	0.79	3.67
	${\varepsilon_{\text{trk}}}^{(2)}$	0.34	3.67	0.61	1.76	1.68
	${\varepsilon_{\text{id}}}^{(1)}$	0.38	0.28	1.72	0.29	1.73
	${\varepsilon_{\text{id}}}^{(2)}$	0.78	0.18	0.56	0.03	0.09
Total ε_{rec}		1.47	4.21	4.73	2.08	6.15
ε_{sel}	ε_{kin}	–	1.04	2.89	–	1.91
	$\varepsilon_{I_{p_{\text{T}}}}$	1.79	1.91	3.19	1.65	2.75
	$\varepsilon_{\lvert\Delta\Phi\rvert}$	1.08	1.03	1.86	0.60	0.97
	ε_{IPS}	2.70	–	–	1.92	2.85
	$\varepsilon_{A_{p_{\text{T}}}}$	2.03	–	–	–	–
Total ε_{sel}		3.97	2.41	4.69	2.60	4.50
Total systematic		11.13	5.41	7.56	3.88	7.88

Table 2. Systematic uncertainties expressed as a percentage of the cross-section for each $Z \to \tau\tau$ analysis stream. Contributions from acceptance $\mathcal{A}$, branching fractions $\mathcal{B}$, number of background events N_{bkg}, reconstruction efficiencies ε_{rec}, and selection efficiencies ε_{sel} are listed. The superscripts on ${\varepsilon_{\text{trk}}}^{(i)}$ and ${\varepsilon_{\text{id}}}^{(i)}$ indicate the first or second τ lepton decay product candidate. The percentage uncertainties on the cross-section for N_{bkg} are quoted for each individual background, as well as the total background. The efficiency uncertainties are split in a similar fashion.

A graphical summary of the individual final state measurements, the combined measurement, the $Z \to \mu\mu$ measurement of ref. [5], and a theory prediction is shown in figure 2. The theory calculation uses DYNNLO [30] with the MSTW08 next-to-next-leading-order (NNLO) PDF set [24], and is found to be $74.3^{+1.9}_{-2.1}$ pb.

JHEP01(2013)111

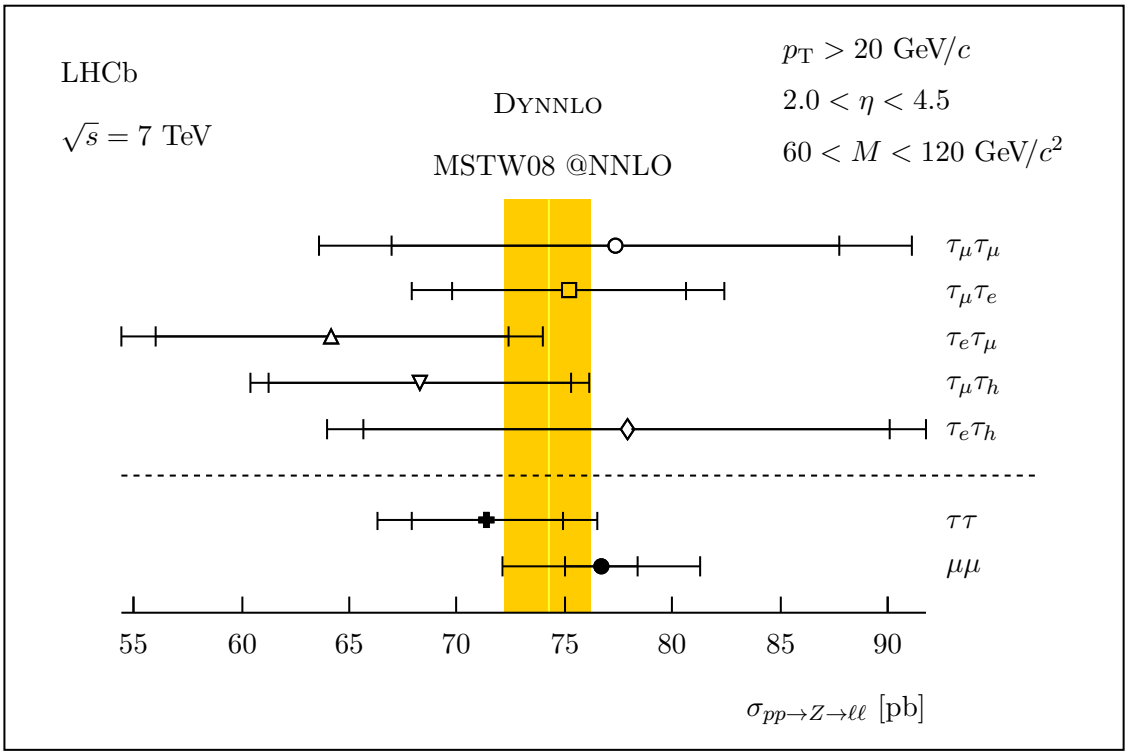

Figure 2. Measured cross-sections for the Z decaying to the final states $\tau_\mu\tau_\mu$, $\tau_\mu\tau_e$, $\tau_e\tau_\mu$, $\tau_\mu\tau_h$, and $\tau_e\tau_h$ (open points) compared with theory (yellow band) and the combined $Z \to \tau\tau$ and LHCb $Z \to \mu\mu$ measurements (closed points) where p_T and η are the transverse momentum and pseudorapidity of the leptons, and M is the di-lepton invariant mass. The inner error bars represent statistical uncertainty while the outer error bars represent combined statistical, systematic, and luminosity uncertainties. The central theory value is given by the light yellow line while the associated uncertainty by the orange band.

The ratio of the combined cross-section to the LHCb $Z \to \mu\mu$ cross-section measurement [5] is found to be

$$\frac{\sigma_{pp\to Z\to\tau\tau}}{\sigma_{pp\to Z\to\mu\mu}} = 0.93 \pm 0.09$$

where the uncertainty is the combined statistical, systematic, and luminosity uncertainties from both measured cross-sections, which are assumed to be uncorrelated.

7 Conclusions

Measurements of inclusive $Z \to \tau\tau$ production in pp collisions at $\sqrt{s} = 7$ TeV in final states containing two muons, a muon and an electron, a muon and a hadron, and an electron and a hadron have been performed using a dataset corresponding to an integrated luminosity of 1028 ± 36 pb^{-1}. The cross-sections for the individual states have been measured in the forward region of $2.0 \leq \eta^\tau \leq 4.5$ with $p_T^\tau > 20$ GeV/c and $60 < M_{\tau\tau} < 120$ GeV/c^2,

JHEP01(2013)111

and a combined result calculated. The results have been compared to Standard Model NNLO theory predictions and with the LHCb $Z \to \mu\mu$ cross-section measurement. The individual measurements, the combined result, the $Z \to \mu\mu$ cross-section, and the theory prediction are all in good agreement. The ratio of the $Z \to \mu\mu$ cross-section to the $Z \to \tau\tau$ cross-section is found to be consistent with lepton universality.

Acknowledgments

We express our gratitude to our colleagues in the CERN accelerator departments for the excellent performance of the LHC. We thank the technical and administrative staff at the LHCb institutes. We acknowledge support from CERN and from the national agencies: CAPES, CNPq, FAPERJ and FINEP (Brazil); NSFC (China); CNRS/IN2P3 and Region Auvergne (France); BMBF, DFG, HGF and MPG (Germany); SFI (Ireland); INFN (Italy); FOM and NWO (The Netherlands); SCSR (Poland); ANCS/IFA (Romania); MinES, Rosatom, RFBR and NRC "Kurchatov Institute" (Russia); MinECo, XuntaGal and GENCAT (Spain); SNSF and SER (Switzerland); NAS Ukraine (Ukraine); STFC (United Kingdom); NSF (U.S.A.). We also acknowledge the support received from the ERC under FP7. The Tier1 computing centres are supported by IN2P3 (France), KIT and BMBF (Germany), INFN (Italy), NWO and SURF (The Netherlands), PIC (Spain), GridPP (United Kingdom). We are thankful for the computing resources put at our disposal by Yandex LLC (Russia), as well as to the communities behind the multiple open source software packages that we depend on.

References

[1] ALEPH, DELPHI, L3, OPAL, SLD, LEP Electroweak Working Group, SLD Electroweak Group, SLD Heavy Flavour Group collaborations, S. Schael et al., *Precision electroweak measurements on the Z resonance*, *Phys. Rept.* **427** (2006) 257 [hep-ex/0509008] [INSPIRE].

[2] J.D. Lykken and K.T. Matchev, *Supersymmetry signatures with τ jets at the Tevatron*, *Phys. Rev.* **D 61** (2000) 015001 [hep-ph/9903238] [INSPIRE].

[3] C.-X. Yue, Y.-M. Zhang and L.-J. Liu, *Nonuniversal gauge bosons Z' and lepton flavor violation τ decays*, *Phys. Lett.* **B 547** (2002) 252 [hep-ph/0209291] [INSPIRE].

[4] W.-F. Chang and J.N. Ng, *Lepton flavor violation in extra dimension models*, *Phys. Rev.* **D 71** (2005) 053003 [hep-ph/0501161] [INSPIRE].

[5] LHCb collaboration, *Inclusive W and Z production in the forward region at $\sqrt{s} = 7$ TeV*, *JHEP* **06** (2012) 058 [arXiv:1204.1620] [INSPIRE].

[6] ATLAS collaboration, *Measurement of the $Z \to \tau\tau$ cross section with the ATLAS detector*, *Phys. Rev.* **D 84** (2011) 112006 [arXiv:1108.2016] [INSPIRE].

JHEP01(2013)111

[7] CMS collaboration, *Measurement of the inclusive Z cross section via decays to τ pairs in pp collisions at $\sqrt{s} = 7$ TeV*, *JHEP* **08** (2011) 117 [arXiv:1104.1617] [INSPIRE].

[8] LHCb collaboration, *The LHCb detector at the LHC*, 2008 *JINST* **3** S08005 [INSPIRE].

[9] S. van der Meer, *Calibration of the effective beam height in the ISR*, CERN-ISR-PO-68-31, CERN, Geneva Switzerland (1968).

[10] M. Ferro-Luzzi, *Proposal for an absolute luminosity determination in colliding beam experiments using vertex detection of beam-gas interactions*, *Nucl. Instrum. Meth.* **A 553** (2005) 388 [INSPIRE].

[11] LHCb collaboration, *Absolute luminosity measurements with the LHCb detector at the LHC*, 2012 *JINST* **7** P01010 [arXiv:1110.2866] [INSPIRE].

[12] I. Belyaev et al., *Handling of the generation of primary events in GAUSS, the LHCb simulation framework*, *IEEE Nucl. Sci. Symp. Conf. Rec.* (2010) 1155.

[13] T. Sjöstrand, S. Mrenna and P.Z. Skands, *PYTHIA* 6.4 *physics and manual*, *JHEP* **05** (2006) 026 [hep-ph/0603175] [INSPIRE].

[14] J. Pumplin et al., *New generation of parton distributions with uncertainties from global QCD analysis*, *JHEP* **07** (2002) 012 [hep-ph/0201195] [INSPIRE].

[15] GEANT4 collaboration, J. Allison et al., GEANT4 *developments and applications*, *IEEE Trans. Nucl. Sci.* **53** (2006) 270 [INSPIRE].

[16] GEANT4 collaboration, S. Agostinelli et al., GEANT4*: a simulation toolkit*, *Nucl. Instrum. Meth.* **A 506** (2003) 250 [INSPIRE].

[17] M. Clemencic et al., *The LHCb simulation application, Gauss: design, evolution and experience*, *J. Phys. Conf. Ser.* **331** (2011) 032023.

[18] LHCb collaboration, A.P. Navarro and M. Frank, *Event reconstruction in the LHCb online cluster*, *J. Phys. Conf. Ser.* **219** (2010) 022020 [INSPIRE].

[19] T. Sjöstrand, S. Mrenna and P.Z. Skands, *A brief introduction to PYTHIA* 8.1, *Comput. Phys. Commun.* **178** (2008) 852 [arXiv:0710.3820] [INSPIRE].

[20] M. Bähr et al., *HERWIG++ physics and manual*, *Eur. Phys. J.* **C 58** (2008) 639 [arXiv:0803.0883] [INSPIRE].

[21] S. Frixione, P. Nason and C. Oleari, *Matching NLO QCD computations with parton shower simulations: the POWHEG method*, *JHEP* **11** (2007) 070 [arXiv:0709.2092] [INSPIRE].

[22] F. Machefert, *LHCb calorimeters and muon system lepton identification*, *AIP Conf. Proc.* **722** (2004) 123.

[23] CTEQ collaboration, H. Lai et al., *Global QCD analysis of parton structure of the nucleon: CTEQ5 parton distributions*, *Eur. Phys. J.* **C 12** (2000) 375 [hep-ph/9903282] [INSPIRE].

[24] A. Martin, W. Stirling, R. Thorne and G. Watt, *Parton distributions for the LHC*, *Eur. Phys. J.* **C 63** (2009) 189 [arXiv:0901.0002] [INSPIRE].

[25] PARTICLE DATA GROUP collaboration, J. Beringer et al., *Review of particle physics*, *Phys. Rev.* **D 86** (2012) 010001 [INSPIRE].

[26] LHCb collaboration, *Measurement of the cross-section for $Z^0 \to e^+e^-$ production in pp collisions at $\sqrt{s} = 7$ TeV*, LHCb-CONF-2012-011, CERN, Geneva Switzerland (2012).

JHEP01(2013)111

[27] T. Skwarnicki, *A study of the radiative cascade transitions between the Υ' and Υ resonances*, Ph.D. thesis, Institute of Nuclear Physics, Krakow Poland (1986) [DESY-F31-86-02] [INSPIRE].

[28] A. Jaeger et al., *Measurement of the track finding efficiency*, LHCb-PUB-2011-025, CERN, Geneva Switzerland (2011).

[29] L. Lyons, D. Gibaut and P. Clifford, *How to combine correlated estimates of a single physical quantity*, *Nucl. Instrum. Meth.* **A 270** (1988) 110 [INSPIRE].

[30] S. Catani and M. Grazzini, *An NNLO subtraction formalism in hadron collisions and its application to Higgs boson production at the LHC*, *Phys. Rev. Lett.* **98** (2007) 222002 [hep-ph/0703012] [INSPIRE].

JHEP01(2013)111

The LHCb collaboration

R. Aaij[38], C. Abellan Beteta[33,n], A. Adametz[11], B. Adeva[34], M. Adinolfi[43], C. Adrover[6], A. Affolder[49], Z. Ajaltouni[5], J. Albrecht[35], F. Alessio[35], M. Alexander[48], S. Ali[38], G. Alkhazov[27], P. Alvarez Cartelle[34], A.A. Alves Jr[22], S. Amato[2], Y. Amhis[36], L. Anderlini[17,f], J. Anderson[37], R.B. Appleby[51], O. Aquines Gutierrez[10], F. Archilli[18,35], A. Artamonov [32], M. Artuso[53], E. Aslanides[6], G. Auriemma[22,m], S. Bachmann[11], J.J. Back[45], C. Baesso[54], W. Baldini[16], R.J. Barlow[51], C. Barschel[35], S. Barsuk[7], W. Barter[44], A. Bates[48], Th. Bauer[38], A. Bay[36], J. Beddow[48], I. Bediaga[1], S. Belogurov[28], K. Belous[32], I. Belyaev[28], E. Ben-Haim[8], M. Benayoun[8], G. Bencivenni[18], S. Benson[47], J. Benton[43], A. Berezhnoy[29], R. Bernet[37], M.-O. Bettler[44], M. van Beuzekom[38], A. Bien[11], S. Bifani[12], T. Bird[51], A. Bizzeti[17,h], P.M. Bjørnstad[51], T. Blake[35], F. Blanc[36], C. Blanks[50], J. Blouw[11], S. Blusk[53], A. Bobrov[31], V. Bocci[22], A. Bondar[31], N. Bondar[27], W. Bonivento[15], S. Borghi[48,51], A. Borgia[53], T.J.V. Bowcock[49], C. Bozzi[16], T. Brambach[9], J. van den Brand[39], J. Bressieux[36], D. Brett[51], M. Britsch[10], T. Britton[53], N.H. Brook[43], H. Brown[49], A. Büchler-Germann[37], I. Burducea[26], A. Bursche[37], J. Buytaert[35], S. Cadeddu[15], O. Callot[7], M. Calvi[20,j], M. Calvo Gomez[33,n], A. Camboni[33], P. Campana[18,35], A. Carbone[14,c], G. Carboni[21,k], R. Cardinale[19,i], A. Cardini[15], H. Carranza-Mejia[47], L. Carson[50], K. Carvalho Akiba[2], G. Casse[49], M. Cattaneo[35], Ch. Cauet[9], M. Charles[52], Ph. Charpentier[35], P. Chen[3,36], N. Chiapolini[37], M. Chrzaszcz [23], K. Ciba[35], X. Cid Vidal[34], G. Ciezarek[50], P.E.L. Clarke[47], M. Clemencic[35], H.V. Cliff[44], J. Closier[35], C. Coca[26], V. Coco[38], J. Cogan[6], E. Cogneras[5], P. Collins[35], A. Comerma-Montells[33], A. Contu[52,15], A. Cook[43], M. Coombes[43], G. Corti[35], B. Couturier[35], G.A. Cowan[36], D. Craik[45], S. Cunliffe[50], R. Currie[47], C. D'Ambrosio[35], P. David[8], P.N.Y. David[38], I. De Bonis[4], K. De Bruyn[38], S. De Capua[51], M. De Cian[37], J.M. De Miranda[1], L. De Paula[2], P. De Simone[18], D. Decamp[4], M. Deckenhoff[9], H. Degaudenzi[36,35], L. Del Buono[8], C. Deplano[15], D. Derkach[14], O. Deschamps[5], F. Dettori[39], A. Di Canto[11], J. Dickens[44], H. Dijkstra[35], P. Diniz Batista[1], M. Dogaru[26], F. Domingo Bonal[33,n], S. Donleavy[49], F. Dordei[11], A. Dosil Suárez[34], D. Dossett[45], A. Dovbnya[40], F. Dupertuis[36], R. Dzhelyadin[32], A. Dziurda[23], A. Dzyuba[27], S. Easo[46,35], U. Egede[50], V. Egorychev[28], S. Eidelman[31], D. van Eijk[38], S. Eisenhardt[47], R. Ekelhof[9], L. Eklund[48], I. El Rifai[5], Ch. Elsasser[37], D. Elsby[42], A. Falabella[14,e], C. Färber[11], G. Fardell[47], C. Farinelli[38], S. Farry[12], V. Fave[36], V. Fernandez Albor[34], F. Ferreira Rodrigues[1], M. Ferro-Luzzi[35], S. Filippov[30], C. Fitzpatrick[35], M. Fontana[10], F. Fontanelli[19,i], R. Forty[35], O. Francisco[2], M. Frank[35], C. Frei[35], M. Frosini[17,f], S. Furcas[20], A. Gallas Torreira[34], D. Galli[14,c], M. Gandelman[2], P. Gandini[52], Y. Gao[3], J-C. Garnier[35], J. Garofoli[53], P. Garosi[51], J. Garra Tico[44], L. Garrido[33], C. Gaspar[35], R. Gauld[52], E. Gersabeck[11], M. Gersabeck[35], T. Gershon[45,35], Ph. Ghez[4], V. Gibson[44], V.V. Gligorov[35], C. Göbel[54], D. Golubkov[28], A. Golutvin[50,28,35], A. Gomes[2], H. Gordon[52], M. Grabalosa Gándara[33], R. Graciani Diaz[33], L.A. Granado Cardoso[35], E. Graugés[33], G. Graziani[17], A. Grecu[26], E. Greening[52], S. Gregson[44], O. Grünberg[55], B. Gui[53], E. Gushchin[30], Yu. Guz[32], T. Gys[35], C. Hadjivasiliou[53], G. Haefeli[36], C. Haen[35], S.C. Haines[44], S. Hall[50], T. Hampson[43], S. Hansmann-Menzemer[11], N. Harnew[52], S.T. Harnew[43], J. Harrison[51], P.F. Harrison[45], T. Hartmann[55], J. He[7], V. Heijne[38], K. Hennessy[49], P. Henrard[5], J.A. Hernando Morata[34], E. van Herwijnen[35], E. Hicks[49], D. Hill[52], M. Hoballah[5], P. Hopchev[4], W. Hulsbergen[38], P. Hunt[52], T. Huse[49], N. Hussain[52], D. Hutchcroft[49], D. Hynds[48], V. Iakovenko[41], P. Ilten[12], J. Imong[43], R. Jacobsson[35], A. Jaeger[11], M. Jahjah Hussein[5], E. Jans[38], F. Jansen[38], P. Jaton[36], B. Jean-Marie[7], F. Jing[3], M. John[52], D. Johnson[52], C.R. Jones[44], B. Jost[35], M. Kaballo[9], S. Kandybei[40], M. Karacson[35], T.M. Karbach[35], I.R. Kenyon[42], U. Kerzel[35], T. Ketel[39], A. Keune[36], B. Khanji[20], Y.M. Kim[47], O. Kochebina[7], V. Komarov[36,29], R.F. Koopman[39], P. Koppenburg[38], M. Korolev[29],

JHEP01(2013)111

A. Kozlinskiy[38], L. Kravchuk[30], K. Kreplin[11], M. Kreps[45], G. Krocker[11], P. Krokovny[31], F. Kruse[9], M. Kucharczyk[20,23,j], V. Kudryavtsev[31], T. Kvaratskheliya[28,35], V.N. La Thi[36], D. Lacarrere[35], G. Lafferty[51], A. Lai[15], D. Lambert[47], R.W. Lambert[39], E. Lanciotti[35], G. Lanfranchi[18,35], C. Langenbruch[35], T. Latham[45], C. Lazzeroni[42], R. Le Gac[6], J. van Leerdam[38], J.-P. Lees[4], R. Lefèvre[5], A. Leflat[29,35], J. Lefrançois[7], O. Leroy[6], T. Lesiak[23], Y. Li[3], L. Li Gioi[5], M. Liles[49], R. Lindner[35], C. Linn[11], B. Liu[3], G. Liu[35], J. von Loeben[20], J.H. Lopes[2], E. Lopez Asamar[33], N. Lopez-March[36], H. Lu[3], J. Luisier[36], H. Luo[47], A. Mac Raighne[48], F. Machefert[7], I.V. Machikhiliyan[4,28], F. Maciuc[26], O. Maev[27,35], J. Magnin[1], M. Maino[20], S. Malde[52], G. Manca[15,d], G. Mancinelli[6], N. Mangiafave[44], U. Marconi[14], R. Märki[36], J. Marks[11], G. Martellotti[22], A. Martens[8], L. Martin[52], A. Martín Sánchez[7], M. Martinelli[38], D. Martinez Santos[35], D. Martins Tostes[2], A. Massafferri[1], R. Matev[35], Z. Mathe[35], C. Matteuzzi[20], M. Matveev[27], E. Maurice[6], A. Mazurov[16,30,35,e], J. McCarthy[42], G. McGregor[51], R. McNulty[12], M. Meissner[11], M. Merk[38], J. Merkel[9], D.A. Milanes[13], M.-N. Minard[4], J. Molina Rodriguez[54], S. Monteil[5], D. Moran[51], P. Morawski[23], R. Mountain[53], I. Mous[38], F. Muheim[47], K. Müller[37], R. Muresan[26], B. Muryn[24], B. Muster[36], J. Mylroie-Smith[49], P. Naik[43], T. Nakada[36], R. Nandakumar[46], I. Nasteva[1], M. Needham[47], N. Neufeld[35], A.D. Nguyen[36], T.D. Nguyen[36], C. Nguyen-Mau[36,o], M. Nicol[7], V. Niess[5], N. Nikitin[29], T. Nikodem[11], A. Nomerotski[52,35], A. Novoselov[32], A. Oblakowska-Mucha[24], V. Obraztsov[32], S. Oggero[38], S. Ogilvy[48], O. Okhrimenko[41], R. Oldeman[15,d,35], M. Orlandea[26], J.M. Otalora Goicochea[2], P. Owen[50], B.K. Pal[53], A. Palano[13,b], M. Palutan[18], J. Panman[35], A. Papanestis[46], M. Pappagallo[48], C. Parkes[51], C.J. Parkinson[50], G. Passaleva[17], G.D. Patel[49], M. Patel[50], G.N. Patrick[46], C. Patrignani[19,i], C. Pavel-Nicorescu[26], A. Pazos Alvarez[34], A. Pellegrino[38], G. Penso[22,l], M. Pepe Altarelli[35], S. Perazzini[14,c], D.L. Perego[20,j], E. Perez Trigo[34], A. Pérez-Calero Yzquierdo[33], P. Perret[5], M. Perrin-Terrin[6], G. Pessina[20], K. Petridis[50], A. Petrolini[19,i], A. Phan[53], E. Picatoste Olloqui[33], B. Pie Valls[33], B. Pietrzyk[4], T. Pilař[45], D. Pinci[22], S. Playfer[47], M. Plo Casasus[34], F. Polci[8], G. Polok[23], A. Poluektov[45,31], E. Polycarpo[2], D. Popov[10], B. Popovici[26], C. Potterat[33], A. Powell[52], J. Prisciandaro[36], V. Pugatch[41], A. Puig Navarro[36], W. Qian[4], J.H. Rademacker[43], B. Rakotomiaramanana[36], M.S. Rangel[2], I. Raniuk[40], N. Rauschmayr[35], G. Raven[39], S. Redford[52], M.M. Reid[45], A.C. dos Reis[1], S. Ricciardi[46], A. Richards[50], K. Rinnert[49], V. Rives Molina[33], D.A. Roa Romero[5], P. Robbe[7], E. Rodrigues[48,51], P. Rodriguez Perez[34], G.J. Rogers[44], S. Roiser[35], V. Romanovsky[32], A. Romero Vidal[34], J. Rouvinet[36], T. Ruf[35], H. Ruiz[33], G. Sabatino[22,k], J.J. Saborido Silva[34], N. Sagidova[27], P. Sail[48], B. Saitta[15,d], C. Salzmann[37], B. Sanmartin Sedes[34], M. Sannino[19,i], R. Santacesaria[22], C. Santamarina Rios[34], R. Santinelli[35], E. Santovetti[21,k], M. Sapunov[6], A. Sarti[18,l], C. Satriano[22,m], A. Satta[21], M. Savrie[16,e], P. Schaack[50], M. Schiller[39], H. Schindler[35], S. Schleich[9], M. Schlupp[9], M. Schmelling[10], B. Schmidt[35], O. Schneider[36], A. Schopper[35], M.-H. Schune[7], R. Schwemmer[35], B. Sciascia[18], A. Sciubba[18,l], M. Seco[34], A. Semennikov[28], K. Senderowska[24], I. Sepp[50], N. Serra[37], J. Serrano[6], P. Seyfert[11], M. Shapkin[32], I. Shapoval[40,35], P. Shatalov[28], Y. Shcheglov[27], T. Shears[49,35], L. Shekhtman[31], O. Shevchenko[40], V. Shevchenko[28], A. Shires[50], R. Silva Coutinho[45], T. Skwarnicki[53], N.A. Smith[49], E. Smith[52,46], M. Smith[51], K. Sobczak[5], F.J.P. Soler[48], F. Soomro[18,35], D. Souza[43], B. Souza De Paula[2], B. Spaan[9], A. Sparkes[47], P. Spradlin[48], F. Stagni[35], S. Stahl[11], O. Steinkamp[37], S. Stoica[26], S. Stone[53], B. Storaci[38], M. Straticiuc[26], U. Straumann[37], V.K. Subbiah[35], S. Swientek[9], M. Szczekowski[25], P. Szczypka[36,35], T. Szumlak[24], S. T'Jampens[4], M. Teklishyn[7], E. Teodorescu[26], F. Teubert[35], C. Thomas[52], E. Thomas[35], J. van Tilburg[11], V. Tisserand[4], M. Tobin[37], S. Tolk[39], D. Tonelli[35], S. Topp-Joergensen[52], N. Torr[52], E. Tournefier[4,50], S. Tourneur[36], M.T. Tran[36], A. Tsaregorodtsev[6], P. Tsopelas[38], N. Tuning[38], M. Ubeda Garcia[35], A. Ukleja[25], D. Urner[51],

JHEP01(2013)111

U. Uwer[11], V. Vagnoni[14], G. Valenti[14], R. Vazquez Gomez[33], P. Vazquez Regueiro[34], S. Vecchi[16], J.J. Velthuis[43], M. Veltri[17,g], G. Veneziano[36], M. Vesterinen[35], B. Viaud[7], I. Videau[7], D. Vieira[2], X. Vilasis-Cardona[33,n], J. Visniakov[34], A. Vollhardt[37], D. Volyanskyy[10], D. Voong[43], A. Vorobyev[27], V. Vorobyev[31], C. Voß[55], H. Voss[10], R. Waldi[55], R. Wallace[12], S. Wandernoth[11], J. Wang[53], D.R. Ward[44], N.K. Watson[42], A.D. Webber[51], D. Websdale[50], M. Whitehead[45], J. Wicht[35], D. Wiedner[11], L. Wiggers[38], G. Wilkinson[52], M.P. Williams[45,46], M. Williams[50,p], F.F. Wilson[46], J. Wishahi[9], M. Witek[23], W. Witzeling[35], S.A. Wotton[44], S. Wright[44], S. Wu[3], K. Wyllie[35], Y. Xie[47,35], F. Xing[52], Z. Xing[53], Z. Yang[3], R. Young[47], X. Yuan[3], O. Yushchenko[32], M. Zangoli[14], M. Zavertyaev[10,a], F. Zhang[3], L. Zhang[53], W.C. Zhang[12], Y. Zhang[3], A. Zhelezov[11], L. Zhong[3], A. Zvyagin[35].

[1] *Centro Brasileiro de Pesquisas Físicas (CBPF), Rio de Janeiro, Brazil*
[2] *Universidade Federal do Rio de Janeiro (UFRJ), Rio de Janeiro, Brazil*
[3] *Center for High Energy Physics, Tsinghua University, Beijing, China*
[4] *LAPP, Université de Savoie, CNRS/IN2P3, Annecy-Le-Vieux, France*
[5] *Clermont Université, Université Blaise Pascal, CNRS/IN2P3, LPC, Clermont-Ferrand, France*
[6] *CPPM, Aix-Marseille Université, CNRS/IN2P3, Marseille, France*
[7] *LAL, Université Paris-Sud, CNRS/IN2P3, Orsay, France*
[8] *LPNHE, Université Pierre et Marie Curie, Université Paris Diderot, CNRS/IN2P3, Paris, France*
[9] *Fakultät Physik, Technische Universität Dortmund, Dortmund, Germany*
[10] *Max-Planck-Institut für Kernphysik (MPIK), Heidelberg, Germany*
[11] *Physikalisches Institut, Ruprecht-Karls-Universität Heidelberg, Heidelberg, Germany*
[12] *School of Physics, University College Dublin, Dublin, Ireland*
[13] *Sezione INFN di Bari, Bari, Italy*
[14] *Sezione INFN di Bologna, Bologna, Italy*
[15] *Sezione INFN di Cagliari, Cagliari, Italy*
[16] *Sezione INFN di Ferrara, Ferrara, Italy*
[17] *Sezione INFN di Firenze, Firenze, Italy*
[18] *Laboratori Nazionali dell'INFN di Frascati, Frascati, Italy*
[19] *Sezione INFN di Genova, Genova, Italy*
[20] *Sezione INFN di Milano Bicocca, Milano, Italy*
[21] *Sezione INFN di Roma Tor Vergata, Roma, Italy*
[22] *Sezione INFN di Roma La Sapienza, Roma, Italy*
[23] *Henryk Niewodniczanski Institute of Nuclear Physics Polish Academy of Sciences, Kraków, Poland*
[24] *AGH University of Science and Technology, Kraków, Poland*
[25] *National Center for Nuclear Research (NCBJ), Warsaw, Poland*
[26] *Horia Hulubei National Institute of Physics and Nuclear Engineering, Bucharest-Magurele, Romania*
[27] *Petersburg Nuclear Physics Institute (PNPI), Gatchina, Russia*
[28] *Institute of Theoretical and Experimental Physics (ITEP), Moscow, Russia*
[29] *Institute of Nuclear Physics, Moscow State University (SINP MSU), Moscow, Russia*
[30] *Institute for Nuclear Research of the Russian Academy of Sciences (INR RAN), Moscow, Russia*
[31] *Budker Institute of Nuclear Physics (SB RAS) and Novosibirsk State University, Novosibirsk, Russia*
[32] *Institute for High Energy Physics (IHEP), Protvino, Russia*
[33] *Universitat de Barcelona, Barcelona, Spain*
[34] *Universidad de Santiago de Compostela, Santiago de Compostela, Spain*
[35] *European Organization for Nuclear Research (CERN), Geneva, Switzerland*
[36] *Ecole Polytechnique Fédérale de Lausanne (EPFL), Lausanne, Switzerland*
[37] *Physik-Institut, Universität Zürich, Zürich, Switzerland*
[38] *Nikhef National Institute for Subatomic Physics, Amsterdam, The Netherlands*

JHEP01(2013)111

[39] *Nikhef National Institute for Subatomic Physics and VU University Amsterdam, Amsterdam, The Netherlands*
[40] *NSC Kharkiv Institute of Physics and Technology (NSC KIPT), Kharkiv, Ukraine*
[41] *Institute for Nuclear Research of the National Academy of Sciences (KINR), Kyiv, Ukraine*
[42] *University of Birmingham, Birmingham, United Kingdom*
[43] *H.H. Wills Physics Laboratory, University of Bristol, Bristol, United Kingdom*
[44] *Cavendish Laboratory, University of Cambridge, Cambridge, United Kingdom*
[45] *Department of Physics, University of Warwick, Coventry, United Kingdom*
[46] *STFC Rutherford Appleton Laboratory, Didcot, United Kingdom*
[47] *School of Physics and Astronomy, University of Edinburgh, Edinburgh, United Kingdom*
[48] *School of Physics and Astronomy, University of Glasgow, Glasgow, United Kingdom*
[49] *Oliver Lodge Laboratory, University of Liverpool, Liverpool, United Kingdom*
[50] *Imperial College London, London, United Kingdom*
[51] *School of Physics and Astronomy, University of Manchester, Manchester, United Kingdom*
[52] *Department of Physics, University of Oxford, Oxford, United Kingdom*
[53] *Syracuse University, Syracuse, NY, U.S.A.*
[54] *Pontifícia Universidade Católica do Rio de Janeiro (PUC-Rio), Rio de Janeiro, Brazil, associated to* [2]
[55] *Institut für Physik, Universität Rostock, Rostock, Germany, associated to* [11]
[a] *P.N. Lebedev Physical Institute, Russian Academy of Science (LPI RAS), Moscow, Russia*
[b] *Università di Bari, Bari, Italy*
[c] *Università di Bologna, Bologna, Italy*
[d] *Università di Cagliari, Cagliari, Italy*
[e] *Università di Ferrara, Ferrara, Italy*
[f] *Università di Firenze, Firenze, Italy*
[g] *Università di Urbino, Urbino, Italy*
[h] *Università di Modena e Reggio Emilia, Modena, Italy*
[i] *Università di Genova, Genova, Italy*
[j] *Università di Milano Bicocca, Milano, Italy*
[k] *Università di Roma Tor Vergata, Roma, Italy*
[l] *Università di Roma La Sapienza, Roma, Italy*
[m] *Università della Basilicata, Potenza, Italy*
[n] *LIFAELS, La Salle, Universitat Ramon Llull, Barcelona, Spain*
[o] *Hanoi University of Science, Hanoi, Viet Nam*
[p] *Massachusetts Institute of Technology, Cambridge, MA, U.S.A.*

JHEP01(2013)111